Clinical Epigenetics

RESEARCH

Open Access

SERPINA1 methylation as a novel diagnostic marker for early-stage papillary thyroid carcinoma via MAPK6-AKT/mTOR pathway

Junjie Li[1,2], Haixia Huang[1,3], Yifei Yin[4], Yizhu Mao[1], Mengxia Li[1], Hong Li[5], Chenxia Jiang[6] and Rongxi Yang[1*]

Abstract

Most thyroid nodules can be diagnosed preoperatively by ultrasonography and fine-needle aspiration biopsy. However, accurately differentiating between benign nodules or indolent thyroid tumors and aggressive thyroid cancers remains a significant clinical challenge when the biopsy results are indeterminate. In this study, we aim to explore a novel biomarker to determine the malignancy of thyroid nodules. Fifteen tissue samples from patients with Stage I&II papillary thyroid carcinoma (PTC) and benign thyroid nodule (BTN) were analyzed by EPIC Methylation 850 K and RNA-Sequencing. Altered and inversely correlated methylation and expression in *SERPINA1* gene in PTC was found in the discovery study. PTC-associated *SERPINA1* hypomethylation was further verified by mass spectrometry in case–control studies from two clinical centers (Validation I: 140 PTCs vs. 182 BTNs, ORs ≥ 2.48, and Validation II: 224 PTCs vs. 217 BTNs, ORs ≥ 2.04; $P \leq 3.07E{-}15$, for all measurable CpG sites). Moreover, *SERPINA1* methylation had an outstanding clinical application value to differentiate PTC from BTN (the AUC combining Validation I and Validation II was 0.92). Our study also revealed that the upregulated SERPINA1 could promote cell proliferation, migration and invasion in the PTC cell lines, and thereby facilitate the malignant progression of PTC. Mechanistically, SERPINA1 activated the AKT/mTOR pathway via binding to MAPK6. Intervention targeting either SERPINA1 or MAPK6 has a significant impact on the malignancy of PTC cells. Together, we identified *SERPINA1* methylation as a functional and effective diagnostic marker for PTC and provided a novel epigenetic insight into the etiology of PTC.

Keywords *SERPINA1*, Benign thyroid nodule, Papillary thyroid carcinoma, Thyroid cancer, Diagnosis, DNA methylation

*Correspondence:
Rongxi Yang
rongxiyang@njmu.edu.cn
Full list of author information is available at the end of the article

Graphical abstract

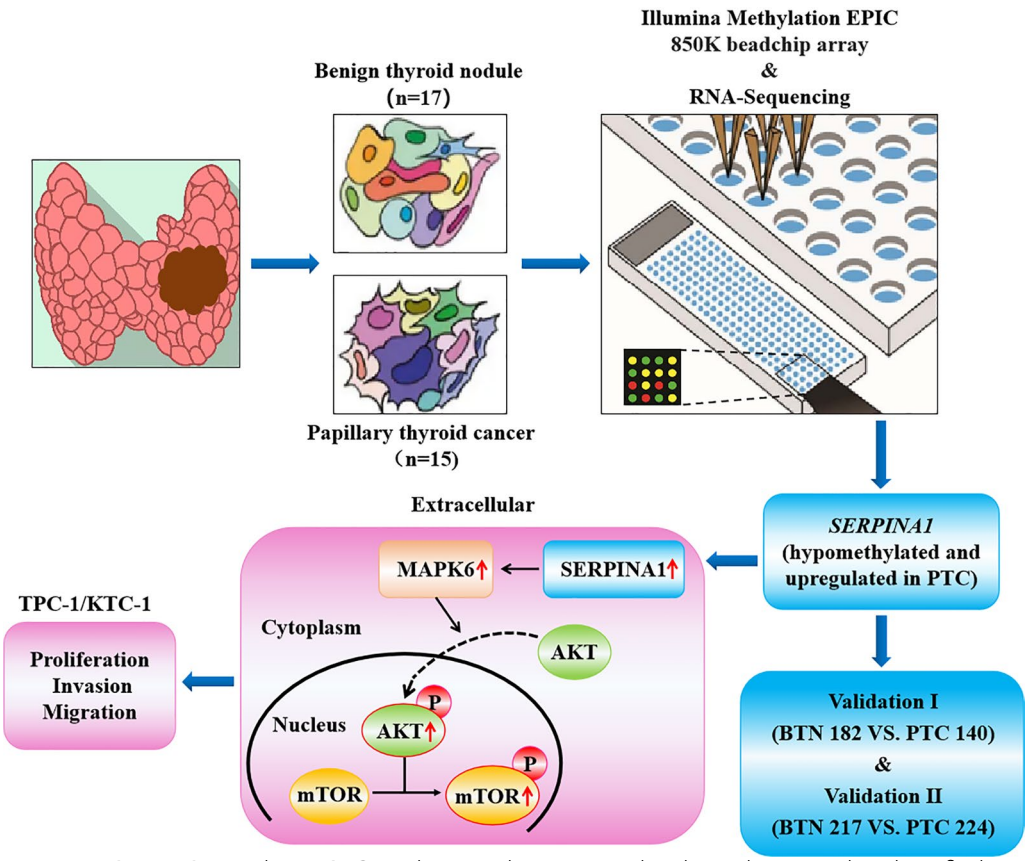

SERPINA1 is a Tumor-Driven Biomarker in PTC. At the population tissue level, we discovered and verified that the methylation level ofSERPINA1 gene wassignificantly decreased and the protein expression was significantly increased in PTC cases, compared toBTN patients. Mechanistically, SERPINA1 significantly activates the AKT/mTOR signaling pathwaythrough binding with MAPK6, which ultimately promotes the malignancy of tumor cells.

Introduction

Thyroid cancer (TC) is the most common endocrine malignancy, especially among older women. Its incidence varies significantly by region, race, age and gender [1]. In recent years, there has been a substantial global rise in the incidence of TC, with an annual growth rate of 20%, posing a serious threat to social economy and human health [2]. Papillary thyroid carcinoma (PTC) with low malignancy and good prognosis is the main pathological subtype of TC, accounting for about 85% of the total cases [3]. A deeper understanding of the occurrence and development of PTC disease is therefore of great importance.

Due to the small size of thyroid gland and abundant peripheral blood vessels, ultrasound-guided Fine needle aspiration biopsy (FNAB) is the principal method and gold standard for preoperative diagnosis of TC in clinical practice. FNAB has little damage to the body and effectively prevents tumor cells dissemination [4]. The Bethesda thyroid cytopathology reporting system categorizes FNAB results into six groups (I–VI) according to cytological characteristics. However, about 20% of thyroid nodules evaluated by FNAB are the Bethesda III–V nodules, which are indeterminate and require further evaluation [5, 6]. In addition, the accuracy of FNAB results largely depends on the experience of pathologists [7]. Therefore, molecular pathological techniques have been developed, such as Afirma® Genomic Sequencing Classifier, ThyroSeq® v3, ThyGenX/ThyraMIR and RosettaGX Reveal, which detect various changes in gene rearrangement, genome mutations or mRNA expression [8, 9]. Nevertheless, the clinical application of these tests is limited by the instability of RNA samples and shared mutations between

malignant and benign thyroid tissues. Hence, reliable and practical biomarkers to distinguish malignant and benign thyroid nodules are urgently needed.

DNA methylation is a common epigenetic modification that affects gene expression. Abnormal DNA methylation has been observed in numerous types of tumors, including TC [10]. For example, oncogene promoter regions are hypomethylated and significantly activated during tumorigenesis [11]. DNA methylation is tissue-specific, highly stable, and can be quantitatively detected. As a potential biomarker, DNA methylation has been widely investigated in the early diagnosis, treatment and prognostic prediction of tumors [12]. Previous reports on differential diagnosis of thyroid nodules mostly focused on DNA methylation of known oncogenes, which had low diagnostic value and lacked external validation of expanded sample size [13]. PTC-specific DNA methylation as a driver in the pathogenesis and malignant progression has been poorly studied.

The activation of mitogen-activated protein kinase (MAPK) signaling pathway has garnered significant attention and is considered to be a key driver in the initiation of PTC. Mutations at site 1799 of the *BRAF* oncogene (*BRAF* V600E), *RAS* mutations or *RET/PTC* rearrangements trigger the activation of the MAPK cascade and phosphatidylinositol-3 kinase (PI3K)/AKT signaling pathway [14, 15]. These over-activated signaling pathways endow tumor cells with strong proliferative, invasion and metastasis ability. The *SERPINA1* gene, located on chromosome 14, encodes a highly conserved and most dominant serine protease inhibitor in humans [16]. Moreover, SERPINA1 plays a role in various biological processes, including angiogenesis, inflammation and tumor metastasis. SERPINA1 has been shown to be significantly upregulated in various cancers, including gastric [17], liver [18] and lung cancers [19]. However, there is no direct evidence to prove the specific regulatory mechanism of *SERPINA1* gene in the occurrence and development of PTC.

Here, we performed the genome-wide DNA methylation and gene expression profiles to discover the DNA methylation alterations in PTC compared to BTN. A significant reduction in *SERPINA1* gene methylation levels in PTC was identified, and then validated by mass spectrometry in case–control studies with a total of 763 patients from two independent clinical centers. The ability of *SERPINA1* methylation in determining the malignancy of thyroid nodules, and its biological function in the pathogenesis and malignant progression of PTC was further evaluated.

Materials and methods

Study population

In the discovery study and two independent validation studies, the inclusion criteria for malignant nodules were as follows: (1) early-stage (stage I–II) PTC with classic papillary structures; (2) no distant metastasis or other simultaneous cancers; (3) no related therapy. BTN patients were matched to PTC cases by age, gender and the year of diagnosis. All cases were histopathologically diagnosed by two qualified pathologists, and clinical TNM stage of each malignant case was determined on the basis of the 8th edition American Joint Committee on Cancer staging system [20].

In the discovery study, a total of 32 fresh-frozen tissue samples were collected from the Second Hospital of Huai'an from 2019 to 2020, including 15 early-stage PTC cases and 17 BTN subjects. All participants were females and had an age range from 23 to 76 years old at diagnosis.

Two independent case–control studies with formalin fixed paraffin embedding (FFPE) tissue samples were conducted for validation. Validation I: 140 early-stage PTCs and 182 age- and gender- matched BTNs were collected from the Second Hospital of Huai'an from 2019 to 2020. Women accounted for 76.43% (107/140) in PTCs and 79.12% (144/182) in BTNs, while men accounted for 23.57% (33/140) in PTCs and 20.88% (38/182) in BTNs. The median ages and interquartile ranges (IQRs) in PTC and BTN groups were 50.00 (43.00–57.00) and 53.00 (46.00–60.25) years old, respectively. ValidationII: a total of 224 early-stage PTCs and 217 age- and gender-matched BTNs were collected from the Nantong Hospital in 2020. Women accounted for 76.34% (171/224) in PTCs and 76.96% (167/217) in BTNs, while men accounted for 23.66% (53/224) in PTCs and 23.04% (50/217) in BTNs. The median ages and interquartile ranges (IQRs) in PTC and BTN groups were 48.00 (34.00–55.00) and 50.00 (37.50–56.00) years old, respectively. The detailed clinical characteristics of the participants, including tumor length, tumor size, involved lymph node, tumor stage, TSH, FT3 and FT4 are shown in Table 1.

The studies were approved by the ethics committee of the Nanjing Medical University. Informed consent was obtained from all patients.

Illumina infinium human methylation EPIC 850 K beadchip array and RNA-sequencing

In the discovery study, according to the manufacturer's instructions, genomic DNA and total RNA were isolated from 32 fresh-frozen tissue samples using FastPure Blood/Cell/Tissue/Bacteria DNA Isolation Mini Kit (DC112, Vazyme, Nanjing, China) and FastPure Cell/Tissue Total RNA Isolation Kit (RC101, Vazyme,

Table 1 Clinical characteristics of the participants in Validations I and II

Variables	Group	Validation I			Validation II		
		BTN (n = 182)	PTC (n = 140)	*P* value	BTN (n = 217)	PTC (n = 224)	*P* value
Age (years)		53.00(46.00–60.25)	50.00(43.00–57.00)	0.054*	50.00(37.50–56.00)	48.00(34.00–55.00)	0.138*
Gender	Female	144(79.12%)	107(76.43%)	0.713$	167(76.96%)	171(76.34%)	0.747$
	Male	38(20.88%)	33(23.57%)		50(23.04%)	53(23.66%)	
Tumor length (cm)		–	1.00(0.90–1.50)		–	1.50(1.10–2.00)	
Tumor size	T1	–	123(87.86%)		–	184(82.14%)	
	T2&3&4	–	17(12.14%)		–	40(17.86%)	
Lymph node involvement	0	–	73(52.14%)		–	78(34.82%)	
	1	–	67(47.86%)		–	146(65.18%)	
Tumor stage	Stage I	–	125(89.29%)		–	187(83.48%)	
	Stage II	–	15(10.71%)		–	37(16.52%)	
TSH (μIU/mL)		1.46(0.90–2.40)	1.89(1.20–3.19)	**0.003***	1.67(1.02–2.46)	2.08(1.45–2.92)	**0.001***
FT3 (pmol/L)		4.47(3.97–5.00)	4.51(3.92–4.98)	0.762*	4.83(4.40–5.26)	4.84(4.30–5.27)	0.968*
FT4 (pmol/L)		16.56(14.57–18.77)	16.35(13.72–18.17)	0.145*	11.23(9.34–12.43)	11.16(9.50–12.29)	0.865*

All *P** values were calculated by Mann–Whitney U test. All *P*$ values were calculated by Chi-square test. Significant *P* values were in bold

Nanjing, China), respectively. Genome-wide DNA methylation profiles were analyzed by using Illumina Infinium Human Methylation EPIC 850 K beadchip array with single-nucleotide resolution. The data were mainly analyzed using ChAMP package in R. The β value was used to represent DNA methylation level / the proportion of methylated each CpG site. First, the probes were filtered with following criteria: detection *P*-value > 0.01, probes with < 3 beads in at least 5% of samples, non-CpG probes, multi-hit probes, probes located in chromosomes X and Y and (SNP-related probes) in turn. Then β value matrix was normalized using BMIQ for adjusting type I and type II probe bias. Next, we used SVA (Singular Value Decomposition Analysis) to analyze the batch effect caused by BeadChip Slide and Array, and applied Combat to correct this batch effect. All the CpG sites were annotated using EPICanno.ilm10b5.hg19. Differential Methylated CpGs Position (probes) were calculated by champ. DMP function, the adj.*P* values were computed using the Benjamini–Hochberg method. Probes meeting the following criteria were considered as differentially methylated: (1) methylation difference (|delta beta| ≥ 0.2) between BTN and PTC groups; (2) an FDR-corrected *P* value < 0.005; (3) no adjacent single-nucleotide polymorphisms (SNPs); (4) in the promoter region, 5'UTR, or the 1st exon of gene body.

Meanwhile, the next generation RNA-sequencing technology was used to detect the levels of mRNA. Paired-end libraries were synthesized by using the Stranded mRNA-seq Lib Prep Kit for Illumina (ABclonal, China) following Preparation Guide. Briefly, the poly-A containing mRNA molecules were purified using poly-T oligo-attached magnetic beads. Following purification, the mRNA is fragmented into small pieces and fragments are copied into first strand cDNA using reverse transcriptase and random primers. This is followed by second strand cDNA synthesis using DNA Polymerase I and RNase H. These cDNA fragments then go through an end repair process, the addition of a single 'A' base, and then ligation of the adapters. The products are then purified and enriched with PCR to create the final cDNA library. Purified libraries were quantified by Qubit® 3.0 Fluorometer (Life Technologies, USA) and validated by Agilent 2100 bioanalyzer (Agilent Technologies, USA) to confirm the insert size and calculate the mole concentration. The cluster was generated by cBot with the library diluted to 10 pM and then were sequenced on the Illumina NovaSeq 6000 (Illumina, USA). Followed by pipeline and quantitative part: paired-end sequence files (fastq) were mapped to the reference genome using Hisat2. The output sequencing alignment map files were converted to BAM (binary alignment/map) files and sorted using SAMtools. Gene abundance was expressed as fragments per kilobase of exon per million reads mapped (FPKM). Stringtie software was used to count the fragment within each gene, and TMM algorithm was used for normalization. Genes mRNA expression with |fold change| ≥ 4 and an FDR-corrected *P* value < 0.005 were thought to be differentially expressed. Through the intersection of 850 K beadchip array and RNA-sequencing data, genes with significant differences in DNA methylation and mRNA were filtered.

Matrix-assisted laser desorption ionization time-of-flight (MALDI-TOF) mass spectrometry

The target sequence of *SERPINA1* amplicon was amplified by polymerase chain reaction (PCR) (Table S2). Upper case letters indicated the sequence specific primer regions, and non-specific tags were shown in lower case letters. The EpiTyper assay detected the methylation levels of eight CpG sites and yielded five distinguishable mass peaks. There were no SNPs located in the primer regions or overlapped with any of the CpG sites in *SERPINA1* amplicon.

DNA methylation was semi-quantitatively analyzed by MALDI-TOF mass spectrometry. All collected PTC and BTN samples were processed in parallel. Firstly, the total DNA was extracted from FFPE tissue samples using Fast Pure FFPE DNA Isolation Kit (DC105, Vazyme, Nanjing, China). Secondly, DNA was treated with sodium bisulfite using EZ-96 DNA Methylation Gold Kit (D5007, Zymo Research, Orange, USA), through which non-methylated cytosine (C) in CpG site was converted to uracil (U), whereas methylated cytosine remained unchanged. Finally, CpG methylation levels of all FFPE tissue samples were measured by mass spectrometry, as described in our previous study [21]. In brief, the target sequence was amplified by PCR. Then, the amplification products were treated with Shrimp Alkaline Phosphatase and followed by T-cleavage using RNase A. After cleaning residual ions with resin, methylation level of each sample was quantified and collected by the Mass ARRAY system.

Cell culture and reagents

Nthy-ori3-1 is human normal thyroid epithelial cell, TPC-1 and KTC-1 are human thyroid papillary carcinoma cells. All cell lines were purchased from the Cell Bank of Shanghai Institutes for Biological Sciences, Chinese Academy of Sciences (Shanghai, China). The cells were cultured in RPMI-1640 medium (Life Technologies/ Gibco, Grand Island, New York) supplemented with 10% FBS, 100 U/mL penicillin and 100 μg/mL streptomycin (Life Technologies/ Gibco, Gaithersburg, MD), and were maintained in 5% CO_2 at 37 °C.

Western blot and co-immunoprecipitation (Co-IP)

Non-reducing RIPA lysis buffer (Beyotime, China) supplemented with protease inhibitors and phosphatase inhibitors were used to extract protein from cells for Western Blot and Co-IP. Equal amounts (60–100 μg) of protein were separated on 10% SDS-PAGE and transferred to polyvinylidene difluoride (PVDF) membranes (Millipore, USA). The membranes were incubated with primary antibodies for GAPDH (Beyotime), SERPINA1 (Abclonal), MAPK6 (Abclonal), AKT (Abclonal), p-AKT (Cell Signaling Technology), mTOR (Abclonal) and p-mTOR (Cell Signaling Technology) overnight at 4 °C. Then, the membranes were incubated with a horseradish peroxidase-conjugated goat-anti-mouse antibody (Beyotime) or a goat-anti-rabbit antibody (Beyotime) for 1 h at room temperature and exposed with ECL reagent (BIO-RAD, USA). Densities of bands were quantified by Image J software. GAPDH levels, measured in parallel, served as controls. Protein–protein interactions in cells were validated by Co-IP, as described previously [22]. The whole experiment was carried out strictly at 4℃. Briefly, 1 μg antibody of the target protein was added to the cell lysate and incubated overnight at 4℃ with shaking slowly. The next day, the pre-treated 10 μl protein A agarose beads were added. For exogenous Co-IP, cells were transfected with the HA-*SERPINA1* or FLAG-*MAPK6* plasmid for 48 h, and then the cells were harvested for protein extraction.

Quantitative real-time PCR (qRT-PCR) analysis

Total RNA from cultured cells was isolated by trizol reagent (Thermo Fisher Scientific, USA) according to the manufacturer's recommendation. The extracted total RNA was then dissolved in 50 μL of RNase-free water and stored at − 80 °C until analysis. To quantitatively detect mRNAs, reverse transcription was performed using 1 μg of total RNA and HiScript II qRT Supermix (Vazyme Biotech) according to the manufacturer's protocol. The real-time PCR was performed using SYBR Green (Fermentas, USA) with a Light Cycler 384 instrument (Roche, Swiss). The $2^{-\Delta\Delta Ct}$ method [23] was used to analyze the qRT-PCR results, and the primer sequences synthesized by TSINGKE are shown in Table S3. GAPDH was used as endogenous control.

Cell transfection

Nthy-ori3-1, TPC-1 and KTC-1 cells were inoculated in 6-well plates and transfected when the cell density reached 50% (siRNA) or 80% (pcDNA). pcDNA-*SERPINA1*, pcDNA-*MAPK6*, pcDNA-Con, *SERPINA1*-siRNA, *MAPK6*-siRNA and si-NC were synthesized by RiBoBio (Guangzhou, China). The cells were transiently transfected by lipofectamine 3000 reagent or in combination with P3000 reagent (Invitrogen, Carlsbad, CA, USA) according to the manufacturer's protocol.

Cell counting Kit-8 (CCK-8), colony formation, wound healing and transwell assays

Cell Counting Kit-8 (WST-8/CCK-8, Beyotime) assay was performed to evaluate cell proliferation. Briefly, 2×10^3 treated cells were inoculated into a 96-well plate (costar® Cell BIND®) and cultured for 0, 24, 48, 72, 96, or 120 h. Then, 10 μL WST-8 was added to each well, and the 96-well plate was read at 460-nm filter absorbance

on a TECAN multifunctional enzyme-labeled instrument (Infinite M200 PRO). The production of formazan is directly proportional to the number of living cells. The results of experiments that were repeated at least three times were analyzed.

After cells were treated as indicated, the 1×10^3 cells were implanted in a 6-well plate (costar® Cell BIND®) containing 2.5 mL medium and cultured for 2 weeks in an incubator maintained in 5% CO_2 and at 37 °C. The colonies were fixed with 4% paraformaldehyde fix solution (Beyotime) and stained with 0.1% crystal violet staining solution (Beyotime), and the colonies between 0.3 and 1.0 mm in diameter were counted.

When cells density reached more than 60% after treatment as indicated, a 10 μL sterile pipette tip was used to vertically scratch the monolingual cells to generate five scratch wounds without changing the tip throughout the process. Then, the non-adherent cells were rinsed with sterile PBS until scratches were clearly visible, and cultured in fresh medium. After 0, 24 and 48 h, the distances between wounds were photographed and measured more than three times, and its average values were calculated.

For invasion experiments, the matrix gel (Matrigel, BD Biosciences, USA) was used to simulate extracellular matrix. The 200 μL serum-free cell suspensions (2.5×10^5 cells /mL) were added to the upper chamber with 8-μm pore filter (Corning, USA) to evaluate migration capacity, and the 100 μL serum-free cell suspensions (1.0×10^6 cells /mL) were added to the upper chamber coated with Matrigel to assess invasion ability. Next, 600 μL complete medium containing 10% FBS was added to the lower chamber as a chemoattractant. After 48 h, the non-migrating and non-invasive cells in the upper chamber were gently wiped off with a cotton swab, and the cells migrated and invaded to the lower chamber were fixed and stained. The cells were observed under an inverted fluorescence microscope at 400×(TE2000, Nikon, China). Five visual fields were randomly selected and photographed, and the average number of cells was calculated. The experiments were conducted in triplicates.

Immunofluorescence

Nthy-ori3-1, TPC-1 and KTC-1 cells were evenly spread in confocal dishes for 24 h, and incubated with primary antibodies for SERPINA1 (Proteintech) and MAPK6 (Abclonal) at 4 °C overnight. Then, the cells were subjected with Cy3-conjugated goat-anti-mouse secondary antibody (Beyotime) and FITC-conjugated goat-anti-rabbit secondary antibody (Beyotime) at room temperature for 1 h in the dark. In addition, 4′,6-diamidino-2-phenylindole (DAPI, Sigma) was added to stain the nucleus for 10 min. The cells were observed under a fluorescence confocal microscope (Zeiss, LSM700B, Germany).

Immunohistochemistry

Fresh tissue samples from patients with early-stage PTCs and benign thyroid nodules (BTNs) were treated with FFPE, and continuously sectioned at 5 μm and placed on glass slides. The tissue sections were deparaffinized, hydrated, and incubated with SERPINA1 (Proteintech) mouse monoclonal antibody. Immunohistochemical evaluation was accomplished by standard methods. Photographs of random fields were taken under a microscope (Nikon TS100, Japan). Positive-staining cells were counted to evaluate the SERPINA1 protein expression, and the levels for SERPINA1 were quantified by Image J software.

Statistical analyses

All data statistical analyses were performed by IBM SPSS Statistics 25.0 version and GraphPad Prism (version 9.0). Non-parametric tests including Mann–Whitney U test and Chi-square test were applied to compare the difference between PTCs and BTNs, and Kruskal–Wallis test was used to compare the methylation levels of clinical characteristics between multiple groups. Binary logistic regression analysis was conducted to calculate odds ratios (ORs) per −10% methylation, and their 95% confidence intervals (95% CIs) were determined after adjusting for age, gender, TSH, FT3 and FT4. Spearman correlation was used to evaluate the correlation between variables. ROC curve was used to evaluate goodness of fit. All tests were two-sided, and a *P* value less than 0.05 was considered to be statistically significant. For the cell experiments, all data were represented as means ± SEM for experiments conducted in triplicate, where * indicating a *P*-value less than 0.05, ** indicating a *P*-value less than 0.01, *** indicating a *P*-value less than 0.001.

Results

Discovery of *SERPINA1* hypomethylation and overexpression in tissues to distinguish early-stage PTC cases from BTN subjects

We performed epigenome-wide screening and whole transcriptome screening for methylation sites and genes with significant differences in 17 BTN and 15 early-stage PTC fresh-frozen tissue samples. We identified that there were 8,368 significantly hypomethylated CpG sites and 5,679 significantly hypermethylated CpG sites in PTCs compared to BTNs (Fig. 1A, B). RNA-Seq data showed that mRNA levels of 1098 genes were significantly upregulated, while mRNA levels of 372 genes were significantly decreased in PTCs compared to BTNs (Fig. 1D, E).

It is well known that alterations in DNA methylation often affect gene expression. Compared to BTN subjects, all the analyzed CpG sites of *SERPINA1* gene (cg16389610 and cg09968361, both located at

the 5'UTR of the *SERPINA1* gene) showed significant hypomethylation in early-stage PTC cases (median methylation value of cg16389610: 0.78 in BTN, and 0.35 in PTC, FDR-corrected *P* value = 0.004; median methylation value of cg09968361: 0.83 in BTN, and 0.58 in PTC, FDR-corrected *P* value = 0.001) (Fig. 1C and Table S1), while the mRNA levels of *SERPINA1* in early-stage PTC cases were significantly increased (median mRNA levels value: 2.14 in BTN and 39.16 in PTC, FDR-corrected *P* value = 6.36E−17) (Fig. 1F and Table S1). Furthermore, there was a significant inverse correlation between the methylation levels of cg16389610 and cg09968361 with the mRNA levels of *SERPINA1*(cg16389610, Spearman's correlation coefficient of −0.82, *P* value = 9.00E−04; cg09968361, Spearman's correlation coefficient of −0.60, *P* value = 2.82E-04) (Fig. 1G and Table S1). Immunohistochemical staining showed that SERPINA1 protein was deposited significantly in PTC cases, and the SERPINA1 positive area was significantly higher than that in BTN subjects (Fig. 1H). Consistently, the TCGA results illustrated that SERPINA1 expression in 512 patients with thyroid cancer (TC) was significantly higher than that in 337 normal controls (N) (FDR-corrected *P* value = 4.70E−117) (Fig. 1I). In addition, the q-PCR result showed that the mRNA level of *SERPINA1* gene was obviously upregulated in PTC cases compared with BTN subjects (Fig. 1J). Similarly, the Western Blot results demonstrated that the SERPINA1 protein was significantly overexpressed in PTC cases compared with BTN subjects (Fig. 1K). In summary, compared with BTN subjects, *SERPINA1* gene is significantly hypomethylated and highly expressed in early-stage PTC cases, suggesting that it may play a crucial role in the occurrence and development of PTC.

Validation of *SERPINA1* hypomethylation in FFPE tissues of PTC by two independent case–control studies.

A 184 bp amplicon (Chr14: 94,855,044–94,855,227 build GRCh37/hg19) was designed on the 5'UTR of *SERPINA1* gene, which covering eight CpG sites including cg16389610 (Chr14: 94,855,202) was designed for further validation by MALDI-TOF mass spectrometry (Fig. 2A). The whole sequence of this cg16389610 amplicon is shown in Table S2, where cg16389610 was referred as CpG_1. The primer designed failed for the amplicon containing cg09968361. Therefore, we focused on the cg16389610 amplicon in the validation study.

Differences in *SERPINA1* methylation between early-stage PTC and BTN were verified with FFPE tissue samples in two independent case–control studies (Validation I and Validation II) (Figure S1A). In Validation I (140 early-stage PTC cases and 182 age- and gender-matched BTN subjects), the CpG_1 methylation levels were the most significantly reduced in PTC cases compared with BTN subjects (methylation values of BTN and PTC: 0.91 vs. 0.52; *P* value = 8.65E−38). Similarly, CpG_2, CpG_3, CpG_4.5 and CpG_7.8 were significantly hypomethylated in PTC cases compared to BTN subjects (methylation values of BTN and PTC, respectively: 0.77 vs. 0.41; 0.80 vs. 0.48; 0.62 vs. 0.39; 0.68 vs. 0.51; all *P* value ≤ 1.19E−22) (Fig. 2B and Table S4). In addition, there was a significant association between *SERPINA1* hypomethylation and the risk of early-stage PTC. After adjusting for age, gender and thyroid-related hormones, the ORs per 10% reduced methylation of all CpG sites in *SERPINA1* amplicon ranged from 2.48 to 3.13 (all *P* values ≤ 3.07E−15; Table S4).

Consistent results were obtained in Validation II (224 early-stage PTC cases and 217 age- and gender-matched BTN subjects). We also observed significant hypomethylation of all CpG sites on *SERPINA1* amplicon in PTC cases compared with BTN subjects. Among them, CpG_1 exhibited the most significantly

(See figure on next page.)

Fig. 1 *SERPINA1* gene is hypomethylated and overexpressed in PTC fresh-frozen tissue samples compared with BTN in the discovery study. Genome-wide DNA methylation and mRNA profiles identify different molecular features between BTN and PTC. **A**, **B** Significant differences in DNA methylation levels between BTN subjects and PTC cases were shown by heat map via hierarchical clustering analysis (**A**) and volcano plot (**B**). The methylation cites of *SERPINA1* gene (cg16389610 and cg09968361) was labeled. **C** Box plots for DNA methylation levels of cg16389610 and cg09968361 in *SERPINA1* gene detected by 850 K beadchip array. **D**, **E** Significant differences in mRNA levels between BTN subjects and PTC cases were shown by heat map via hierarchical clustering analysis (**D**) and volcano plot (**E**). *SERPINA1* was highlighted in bold. **F** Box plots for mRNA levels of *SERPINA1* gene measured by RNA-Sequencing. **G** The correlation coefficient between methylation levels of cg16389610 and cg09968361 and *SERPINA1* mRNA expression was assessed by Spearman's correlation analysis. **H** SERPINA1 protein expression in BTN and PTC tissue sections was evaluated by immunohistochemistry, and quantified by Image J software. Nucleus: blue; Protein deposition: brown. **I** The Cancer Genome Atlas (TCGA) was used to analyze significant differences in SERPINA1 expression levels between human thyroid carcinoma (TC: n = 512) and adjacent pair-matched normal tissues (N: n = 337). **J** The mRNA levels of *SERPINA1* gene in fresh-frozen tissue of BTN subjects and PTC cases were determined by qRT-PCR. **K** The protein expression of SERPINA1 was performed by Western Blot, and the relative protein levels of SERPINA1 were quantitatively determined. Densities of bands were quantified by Image J software. GAPDH served as control. All data are presented as means ± SEM (Standard Error of Mean) for experiments conducted in triplicate

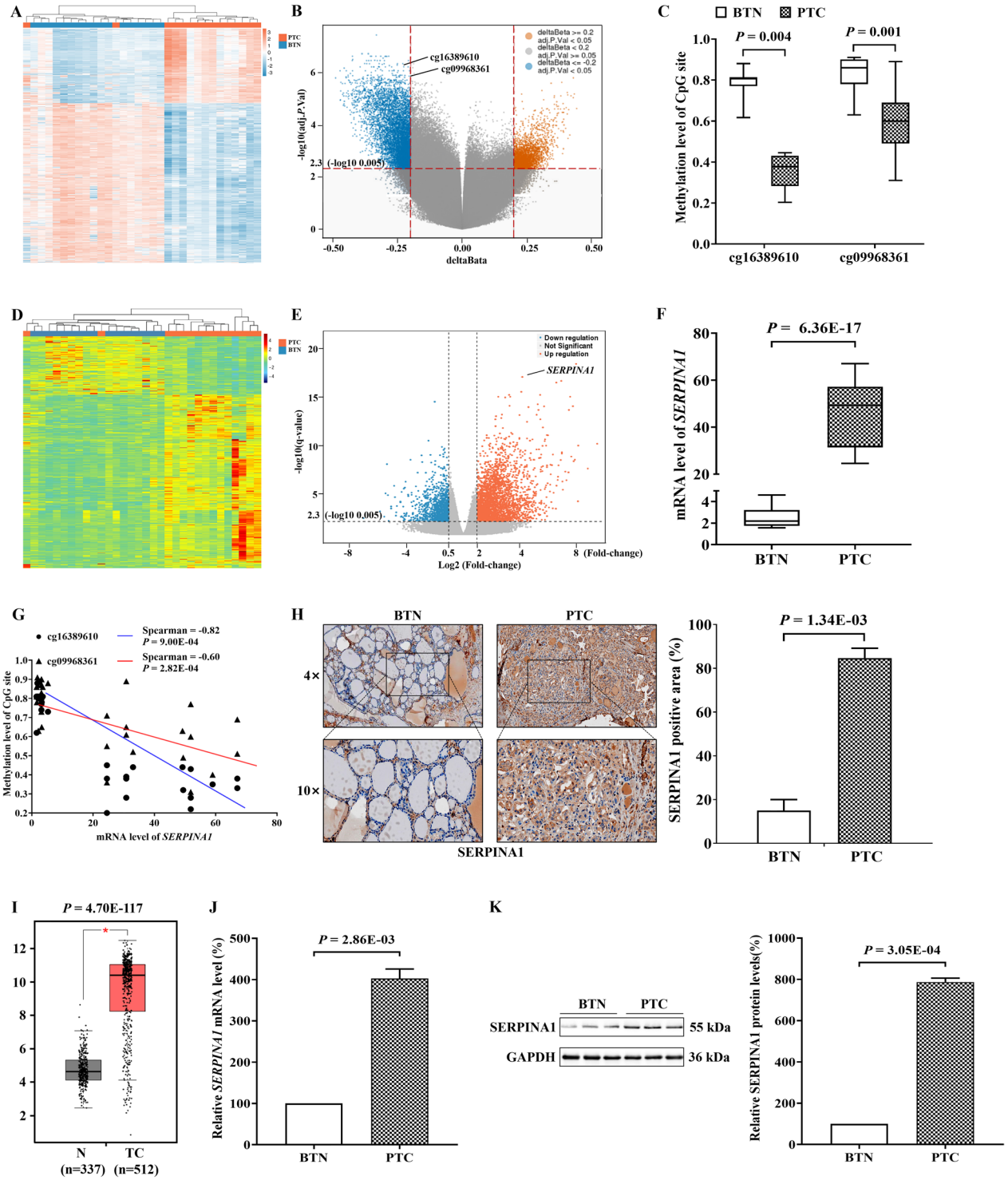

Fig. 1 (See legend on previous page.)

decreased methylation levels in PTC cases compared with BTN subject (methylation values of BTN and PTC: 0.93 vs. 0.45; *P* value = 2.00E−42) (Fig. 2C and Table S4). Moreover, *SERPINA1* hypomethylation had robust association with early-stage PTC, with covariates-adjusted ORs per 10% reduced methylation of each CpG site ranging from 2.04 to 2.43 (all *P* values ≤ 2.58E−19; Table S4).

The association between FFPE tissue-based *SERPINA1* hypomethylation and early-stage PTC stratified by age or gender

To investigate the effects of gender or age on the association between *SERPINA1* hypomethylation and early-stage PTC, while avoiding possible bias due to the small sample size, all subjects from two validations were combined (364 PTC cases vs. 399 BTN subjects) and stratified by gender or age for binary logistic regression analysis. When stratified by gender, for male group, all CpG sites on *SERPINA1* amplicon in PTC cases presented significantly decreased methylation levels compared to BTN subjects (Fig. 2D and Table S5). After adjusting for age and thyroid-related hormones, the ORs per 10% reduced methylation of the seven CpG sites ranged from 2.09 to 2.94 (all *P* values ≤ 1.29E-08; Table S5). Similarly, for female group, the seven CpG sites were significantly hypomethylated in PTC cases than that in BTN subjects (Fig. 2E and Table S5). After adjusting for age and thyroid-related hormones, the ORs per 10% reduced methylation of all CpG sites ranged from 2.23 to 2.74 (all *P* values ≤ 1.41E−25; Table S5). Compared with male group, *SERPINA1* methylation levels and OR values exhibited a greater difference between early-stage PTC cases and BTN subjects in female group, suggesting that the *SERPINA1* hypomethylation was an important risk factor for PTC in female.

In addition, all participants were stratified by the age of 55 years old, which is a cut-off threshold for tumor staging of PTC cases [20]. For age < 55 years old group, the methylation levels of all CpG sites in *SERPINA1* amplicon were significantly decreased in PTC cases compared to BTN subjects (Fig. 2F and Table S6). After adjusting for gender and thyroid-related hormones, the ORs per 10% reduced methylation levels of the seven CpG sites ranged from 2.24 to 2.79 (all *P* values ≤ 1.19E−22; Table S6). Consistently, for age ≥ 55 years old group, the seven CpG sites were significantly hypomethylated in PTC cases than that in BTN subjects (Fig. 2G and Table S6). After adjusting for gender and thyroid-related hormones, the ORs per 10% reduced methylation levels of all CpG sites ranged from 2.13 to 2.58 (all *P* values ≤ 1.37E−12; Table S6). In short, *SERPINA1* hypomethylation as a potential risk factor for PTC works equally well in seniors and young adults.

The diagnostic efficiency of *SERPINA1* hypomethylation in distinguishing early-stage PTC from BTN

The above studies confirmed that *SERPINA1* was significantly hypomethylated in PTC compared to BTN. Next, we performed receiver operating characteristic (ROC) curve and binary logistic regression analysis to further evaluate the potential diagnostic efficiency of *SERPINA1* hypomethylation as a biomarker for PTC. We combined Validation I and Validation II and generated a predicted probability of methylation levels at seven CpG sites within the *SERPINA1* gene. First, the clinical application value of *SERPINA1* methylation was evaluated in all subjects (364 PTC cases vs. 399 BTN subjects), where area under the ROC curve (AUC) was 0.92 (95% CI 0.89–0.95) (Fig. 3A). Subsequently, all subjects from two independent validations were stratified to investigate the effects of age and gender on the clinical value of *SERPINA1* methylation in the differential diagnosis of thyroid nodules. The results showed that the AUC for male and female subjects were 0.92(95% CI 0.89–0.94) and 0.93(95% CI 0.90–0.95), respectively (Fig. 3B,C); the AUC of subjects < 55 years old was 0.93(95% CI 0.91–0.96) and that of subjects ≥ 55 years old was 0.92(95% CI 0.88–0.96) (Fig. 3D,E). As a proto-oncogene, the V600E mutation of the *BRAF* gene is the most common in thyroid cancer. Therefore, we evaluated the efficiency of *BRAF* V600E alone or in combination with *SERPINA1* methylation in the differential diagnosis of thyroid nodules. The results revealed that the combined application of *BRAF* V600E and *SERPINA1* methylation achieved higher diagnostic accuracy (AUC = 0.77(95% CI 0.74–0.81) for *BRAF* V600E alone, and AUC = 0.95(95% CI 0.93–0.96) for combining with *SERPINA1* methylation; Fig. 3F). In short, these results indicated that *SERPINA1* hypomethylation based on FFPE tissue has high confidence and accuracy in distinguishing early-stage PTC from BTN.

(See figure on next page.)

Fig. 2 Validation of *SERPINA1* gene hypomethylation in FFPE tissue samples from PTC cases compared to BTN subjects in two independent case–control studies. **A** Schematic diagram of the target amplicon within *SERPINA1* gene. A 184 bp amplicon covering eight methylated CpG sites was located at 5′-UTR of the *SERPINA1* gene (Chr14: 94,855,044–94,855,227, build GRCh37/hg19, defined by the UCSC Genome Browser). The mass value of the CpG_6 site was too low to be displayed. The cg16389610 was referred to CpG_1. **B**, **C** Box plots for DNA methylation levels of the seven CpG sites within *SERPINA1* amplicon in BTN subjects and PTC cases detected by mass spectrometry in Validation I (B) and Validation II (C). **D**–**G** Combination analysis of the association between *SERPINA1* hypomethylation in all FFPE tissues stratified by age or gender. Box plots for DNA methylation levels of the seven CpG sites within *SERPINA1* amplicon in BTN subjects and PTC cases in male group (D), female group (E), age < 55 years old group (F) and age ≥ 55 years old group (G). All *P* values were calculated by logistic regression with covariates-adjusted

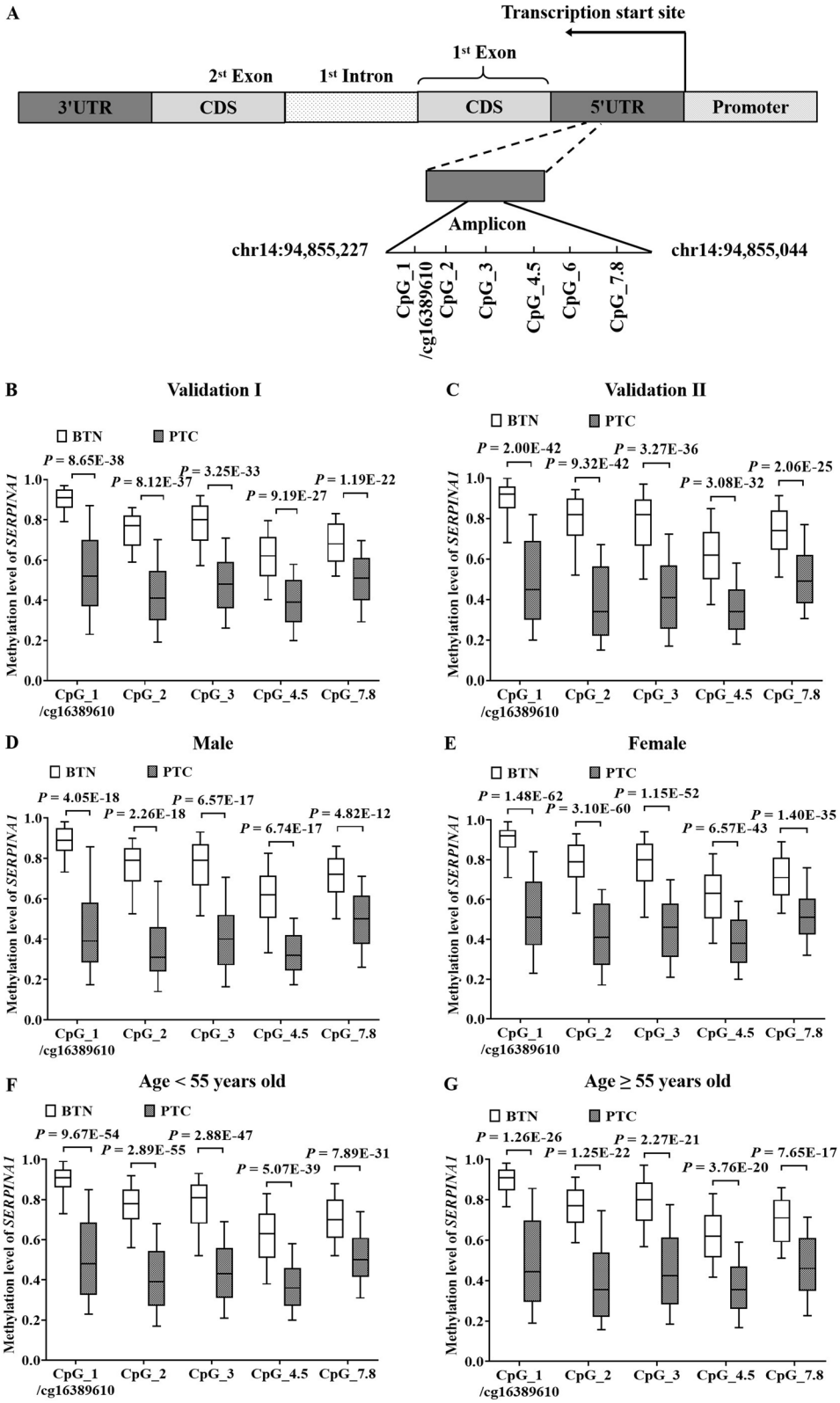

Fig. 2 (See legend on previous page.)

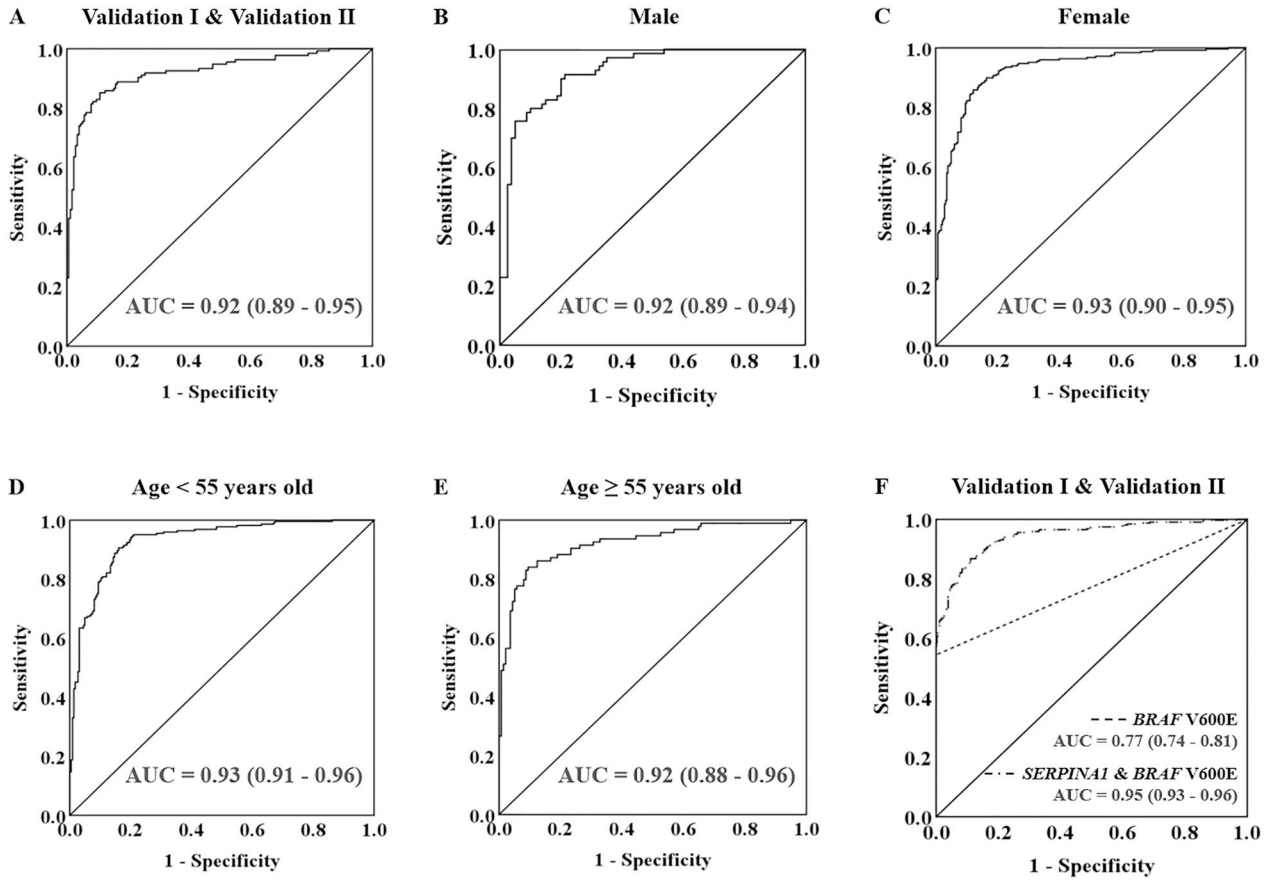

Fig. 3 The diagnostic efficiency of *SERPINA1* hypomethylation in distinguishing early-stage PTC cases from BTN patients. The prediction probability of *SERPINA1* hypomethylation was generated for the methylation levels of seven CpG sites within *SERPINA1* gene. Validation I and Validation II were combined, and stratified by gender or the age of 55 years old. **A** ROC curve analyses for the discriminatory power of *SERPINA1* methylation to distinguish PTC cases from BTN subjects in all FFPE tissue samples. **B**–**E** ROC curve analyses for the discriminatory power of *SERPINA1* methylation to distinguish PTC cases from BTN subjects in male group (B), female group (C), age < 55 years old group (D) and age ≥ 55 years old group (E). **F** ROC curve analysis for the discriminatory power of *BRAF* gene mutation (*BRAF* V600E) or *SERPINA1* methylation in combination with *BRAF* V600E to distinguish PTC cases from BTN subjects in all FFPE tissue samples. The data in panel A-F are presented as AUC (95% confidence interval (CI)). All the 95% CI of AUC were calculated by logistic regression with covariates-adjusted

A comprehensive analysis of the correlation between *SERPINA1* hypomethylation and the clinical characteristics of early-stage PTC

Stratification of 364 early-stage PTC cases from two validations was performed according to clinical characteristics, and non-parametric tests were used to analyze whether *SERPINA1* methylation differences between subgroups were significant. The results showed that methylation levels at CpG_1, CpG_2, CpG_3 and CpG_4.5 sites of *SERPINA1* gene were significantly and negatively correlated with tumor length, tumor size, lymph node involvement and tumor stage, all of which reflected the malignant progression of PTC (all *P* values ≤ 0.050; Table 2). However, for *SERPINA*_CpG_7.8, there was no significant correlation between methylation levels and tumor malignancy characteristics (all *P* values > 0.05; Table 2). In addition, there were no significant correlations between *SERPINA1* methylation and thyroid-related hormones (TSH, FT3 or FT4) (all *P* values ≥ 0.05; Table 2). These results suggested that *SERPINA1* methylation may also be an effective biomarker for determining the malignancy of PTC.

The hypomethylation and overexpression of *SERPINA1* in PTC cells contributes to the malignancy of tumor cells

We next intended to validate the hypomethylation and upregulation of *SERPINA1* gene identified in tissue samples obtained from PTC patients using in vitro cell models. Additionally, we aimed to investigate the role and underlying molecular mechanism of *SERPINA1* gene in the initiation and progression of PTC. Therefore, one normal thyroid epithelial cell line (Nthy-ori3-1) and two PTC cell lines (TPC-1 and KTC-1) were used for functional experiments.

Table 2 The correlation between *SERPINA1* methylation and the clinical characteristics of PTC

Clinical characteristics	Group (n)	Median of methylation levels				
		CpG_1/cg16389610	CpG_2	CpG_3	CpG_4.5	CpG_7.8
Tumor length(cm)	< 1.50 (195)	0.51(0.36–0.75)	0.41(0.28–0.61)	0.48(0.31–0.63)	0.38(0.28–0.51)	0.52(0.40–0.62)
	≥ 1.50 (189)	0.44(0.30–0.68)	0.36(0.23–0.55)	0.42(0.29–0.55)	0.36(0.26–0.46)	0.50(0.39–0.62)
	*P** value	**0.027**	**0.046**	**0.031**	**0.050**	0.459
Tumor size	T1 (298)	0.51(0.35–0.71)	0.41(0.27–0.60)	0.46(0.31–0.60)	0.38(0.28–0.51)	0.51(0.40–0.62)
	T2&3&4 (66)	0.42(0.26–0.66)	0.32(0.20–0.54)	0.41(0.25–0.54)	0.34(0.24–0.44)	0.50(0.37–0.61)
	*P** value	**0.019**	**0.008**	**0.046**	**0.016**	0.295
Lymph node involvement	pN0 (148)	0.56(0.37–0.75)	0.43(0.28–0.59)	0.49(0.34–0.62)	0.40(0.28–0.50)	0.52(0.41–0.62)
	pN1 (213)	0.43(0.31–0.68)	0.36(0.24–0.58)	0.42(0.28–0.55)	0.36(0.26–0.46)	0.50(0.38–0.61)
	*P** value	**0.018**	**0.041**	**0.012**	**0.045**	0.472
Tumor stage	Stage I (312)	0.51(0.34–0.70)	0.40(0.27–0.58)	0.46(0.31–0.59)	0.40(0.29–0.49)	0.51(0.40–0.62)
	Stage II (52)	0.41(0.32–0.71)	0.34(0.25–0.58)	0.41(0.28–0.63)	0.34(0.27–0.43)	0.47(0.36–059)
	*P** value	**0.032**	**0.048**	**0.045**	**0.041**	0.102
TSH (μIU/mL)	< 1.96 (173)	0.46(0.32–0.69)	0.36(0.26–0.56)	0.44(0.29–0.58)	0.35(0.26–0.46)	0.50(0.40–0.61)
	≥ 1.96 (173)	0.52(0.36–0.74)	0.41(0.26–0.61)	0.46(0.31–0.61)	0.39(0.29–0.51)	0.51(0.39–0.62)
	*P** value	0.082	0.144	0.377	0.108	0.471
FT3 (pmol/L)	< 4.72 (173)	0.51(0.37–0.72)	0.41(0.27–0.60)	0.46(0.33–0.62)	0.38(0.28–0.51)	0.51(0.39–0.64)
	≥ 4.72 (173)	0.48(0.31–0.71)	0.37(0.24–0.57)	0.44(0.28–0.58)	0.36(0.27–0.46)	0.50(0.39–0.60)
	*P** value	0.191	0.135	0.331	0.286	0.393
FT4 (pmol/L)	< 12.29 (172)	0.47(0.31–0.69)	0.36(0.24–0.58)	0.42(0.27–0.55)	0.35(0.26–0.45)	0.50(0.39–0.62)
	≥ 12.29 (174)	0.50(0.33–0.71)	0.40(0.27–0.54)	0.46(0.31–0.60)	0.39(0.27–0.50)	0.50(0.39–0.60)
	*P** value	0.500	0.681	0.052	0.101	0.435

All *P** values were calculated by Mann–Whitney U test. Significant *P* values were in bold

The methylation levels at all CpG sites in *SERPINA1* amplicon were significantly down-regulated (Fig. 4A), whereas the mRNA and protein levels of *SERPINA1* were obviously upregulated in TPC-1 and KTC-1 cells compared to Nthy-ori3-1 cells (Fig. 4B,C). Next, Nthy-ori3-1 cells were transfected with overexpressed plasmid or negative control (pcDNA-*SERPINA1* or pcDNA-Con), and TPC-1 and KTC-1 cells were transfected with small interfering RNA or negative control (*SERPINA1*-siRNA or si-NC) (Figure S1B). The transfection efficiency was examined at both mRNA levels by q-PCR (Figure S1C) and protein levels by Western Blot (Fig. 5A). The overexpression of *SERPINA1* gene significantly enhanced the proliferative activity, colony formation, migration and invasion capacities of Nthy-ori3-1 cells. Conversely, knockdown of *SERPINA1* gene significantly inhibited these properties inTPC-1 and KTC-1 cells (Fig. 5B–E). In short, knockdown of *SERPINA1* gene could significantly descend the malignancy of tumor cells, while overexpression of *SERPINA1* gene promoted the malignant transformation of normal thyroid epithelial cells.

SERPINA1 significantly activates the AKT/mTOR signaling pathway by directly binding to MAPK6

Next, we explored the specific regulatory mechanism of SERPINA1 in the initiation and development of PTC. Based on three protein-interacting prediction websites (BioGrid, STRING and HINT), we identified that SERPINA1 exhibits a directly binding affinity to MAPK6 in humans (Fig. 6A). Previous studies have demonstrated that MAPK6 and MAPK4 share the same domain and have very similar biological functions, and both can directly activate the AKT/mTOR signaling pathway to promote tumor growth [24–26]. We found that overexpression of *SERPINA1* gene significantly increased SERPINA1, MAPK6, p-AKT and p-mTOR in Nthy-ori3-1 cells, indicating that the AKT/mTOR signaling pathway was obviously activated. In contrast, knockdown of *SERPINA1* significantly reduced these signaling molecules in TPC-1 and KTC-1 cells, indicating that the AKT/mTOR signaling pathway was strongly inhibited (Fig. 6B, C). Furthermore, immunofluorescence results showed that SERPINA1 and MAPK6 were well colocalized in Nthy-ori3-1, TPC-1 and KTC-1 cells (Fig. 6D). The direct binding between SERPINA1 and MAPK6 was confirmed by endogenous and exogenous Co-IP results (Fig. 6E).

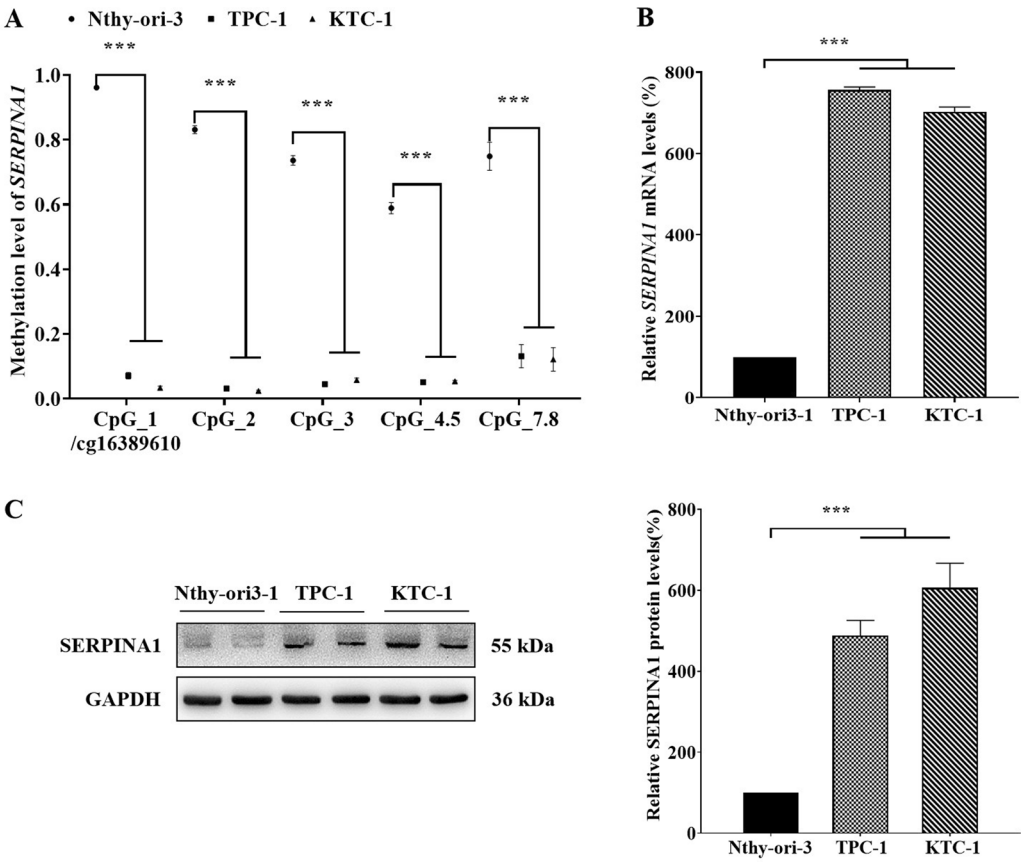

Fig. 4 *SERPINA1* gene is significantly hypomethylated and highly expressed in PTC cell lines. **A** The DNA methylation levels of the seven CpG sites within *SERPINA1* amplicon in Nthy-ori3-1 (normal thyroid epithelial cell line) cells, TPC-1 and KTC-1 (papillary thyroid carcinoma cell lines) cells were quantitatively measured by Mass Spectrometry. **B** The mRNA levels of *SERPINA1* gene of the three cell lines were determined by qRT-PCR. **C** The protein expression of SERPINA1 was detected by Western Blot, and the relative protein levels of SERPINA1 were determined. Densities of bands were quantified by Image J software. GAPDH served as control. All data are presented as means ± SEM for experiments conducted in triplicate. ***$P < 0.001$

SERPINA1/MAPK6/AKT/mTOR signaling pathway enhances the malignancy of PTC cells.

To directly verify that SERPINA1 activates the AKT/mTOR signaling pathway through targeted binding to MAPK6, cell co-transfection experiments were conducted. The transfection efficiency of the cells was measured by q-PCR (Figure S1D). Western Blot results showed that transfection of pcDNA-*SERPINA1* alone significantly increased the expression of SERPINA1, MAPK6, p-AKT and p-mTOR in Nthy-ori3-1 cells, which was significantly reversed when co-transfection of *MAPK6*-siRNA. In contrast, in TPC-1 and KTC-1 cells, the expression of SERPINA1, MAPK6, p-AKT and p-mTOR were significantly decreased by transfection with *SERPINA1*-siRNA alone, which was strongly reversed when co-transfection of pcDNA-*MAPK6* (Fig. 7A,B). Consistently, the proliferation activity, colony formation, migration and invasion capacities of Nthy-ori3-1 cells enhanced by transfection of pcDNA-*SERPINA1* alone was significantly reversed when co-transfecting *MAPK6*-siRNA. Conversely, these properties in TPC-1 and KTC-1 cells weakened by transfection of *SERPINA1*-siRNA alone was strongly reversed when co-transfecting pcDNA-*MAPK6* (Fig. 7C–F). These results suggested that SERPINA1 was involved in the regulation of AKT/mTOR signaling pathway by targeting MAPK6, thereby promoting the occurrence and malignant progression of PTC.

Discussion

In recent years, the detection rate of thyroid nodules under ultrasound guidance has increased rapidly, reaching about 60% [27]. TC accounts for about 5% of the total cases of thyroid nodules, among which PTC is the most common subtype [28]. Although the mortality rate of TC is relatively low, there are still a few subtypes with high malignancy and poor prognosis that seriously endanger patient's life and health [29, 30]. Meanwhile, the increasing incidence of PTC led to a significant increase in the

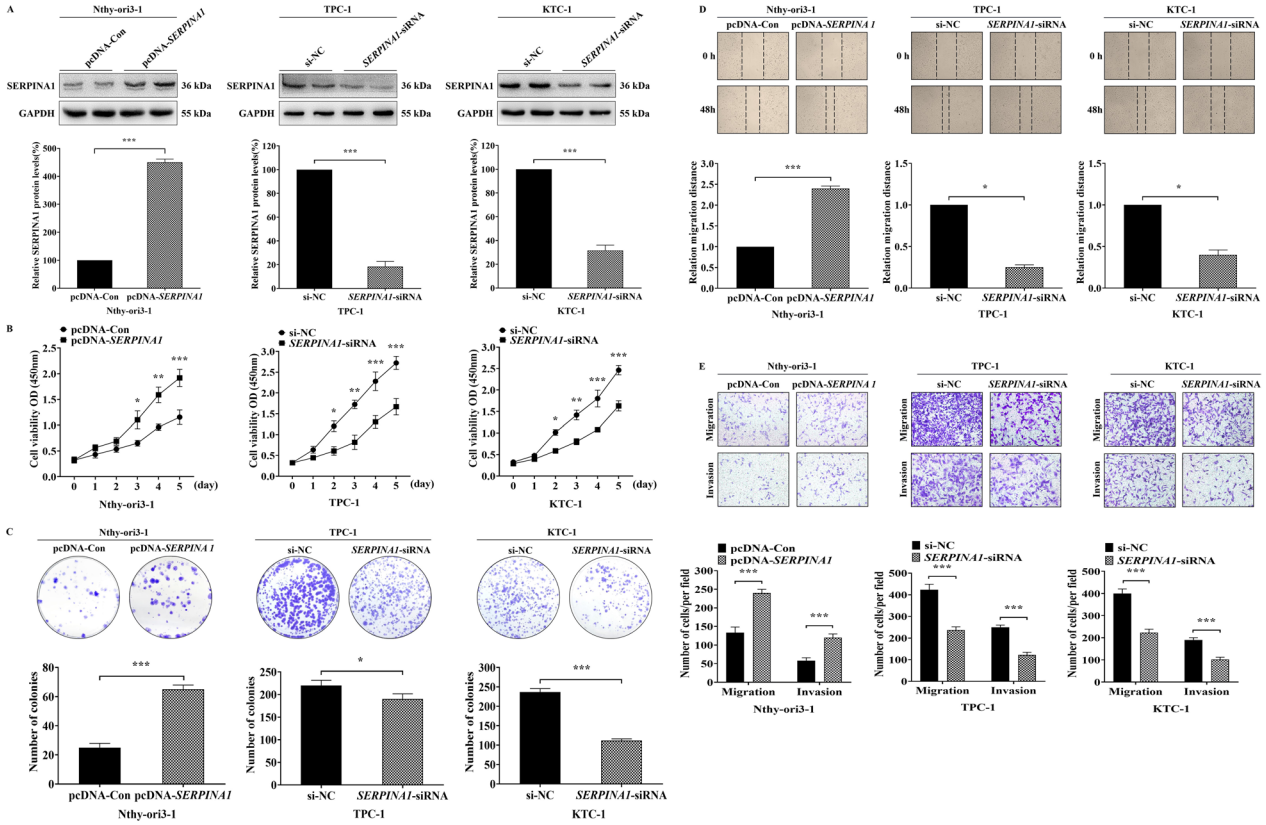

Fig. 5 Knockdown of *SERPINA1* gene significantly inhibits the malignancy of thyroid cancer cells. Nthy-ori3-1 (normal thyroid epithelial cell line) cells were transfected with pcDNA-Con (negative control) or pcDNA-*SERPINA1*, while TPC-1 and KTC-1 (papillary thyroid carcinoma cell lines) cells were transfected with si-NC (negative control) or *SERPINA1*-siRNA. **A** The protein expression of SERPINA1 was examined by Western Blot, and the relative protein levels were determined. Densities of bands were quantified by Image J software. GAPDH served as control. **B** The proliferative activity of Nthy-ori3-1, TPC-1 and KTC-1 cells was measured by the Cell Counting Kit-8 assays. **C** The colony formation ability of cells was evaluated by a 14-day plate cloning experiment and representative pictures of colonies were displayed. Colonies between 0.3 mm and 1.0 mm in diameter were counted. **D** The wound healing and the relative migration distance of cells were determined. (E) The migration and invasion ability of Nthy-ori3-1, TPC-1 and KTC-1 cells were measured by Transwell assays. All data were presented as means ± SEM for experiments conducted in triplicate. **P* < 0.05, ***P* < 0.01, ****P* < 0.001

rate of total thyroidectomy. However, excessive total thyroidectomy may result in serious sequelae, such as intraoperative suffocation, permanent hoarseness, and lifelong use of euthyrox, which not only aggravate the economic burden of patients, but also waste medical resources [31]. Therefore, it is very important to accurately differentiate aggressive PTC cases from benign nodules or inert PTC patients, which can effectively avoid overtreatment.

At present, pathological biopsy and FNAB are the gold standard and most commonly used means for preoperative diagnosis of thyroid nodules [32]. Due to the frequent overlap of cytological features between benign and malignant nodules, and according to the Bethesda Thyroid cytopathology Reporting System, approximately 20% of nodules evaluated via FNAB were still inconclusive Bethesda III–V nodules [33, 34]. It is urgent to find an objective, stable and practical biomarker to accurately distinguish the properties of nodules. Some important human proto-oncogenes, such as *BRAF*, *RAS*, *RET*/*PTC*, have contributed to the development of auxiliary diagnosis [35]. *BRAF* gene mutations are common in a variety of solid tumors, of which V600E mutations account for more than 80% [36]. *BRAF* V600E mutation often leads to persistent activation of MAPK signaling pathway, which ultimately enhances the malignancy of tumor cells [37]. For thyroid diseases, *BRAF* V600E is most closely associated with PTC, with a mutation rate of about 40–70% [38, 39]. The AUC results of this study also confirmed a low diagnostic efficacy of 0.77(0.74–0.81) for *BRAF* V600E mutations across all thyroid nodules. DNA methylation is an emerging biomarker for clinical diagnosis of tumors, including TC [40, 41]. However, only a few studies have focused on the identification of thyroid nodule properties [10, 42]. The present study discovered and validated *SERPINA1* hypomethylation in PTC compared to BTN. Consistently, the mRNA and protein levels of *SERPINA1*

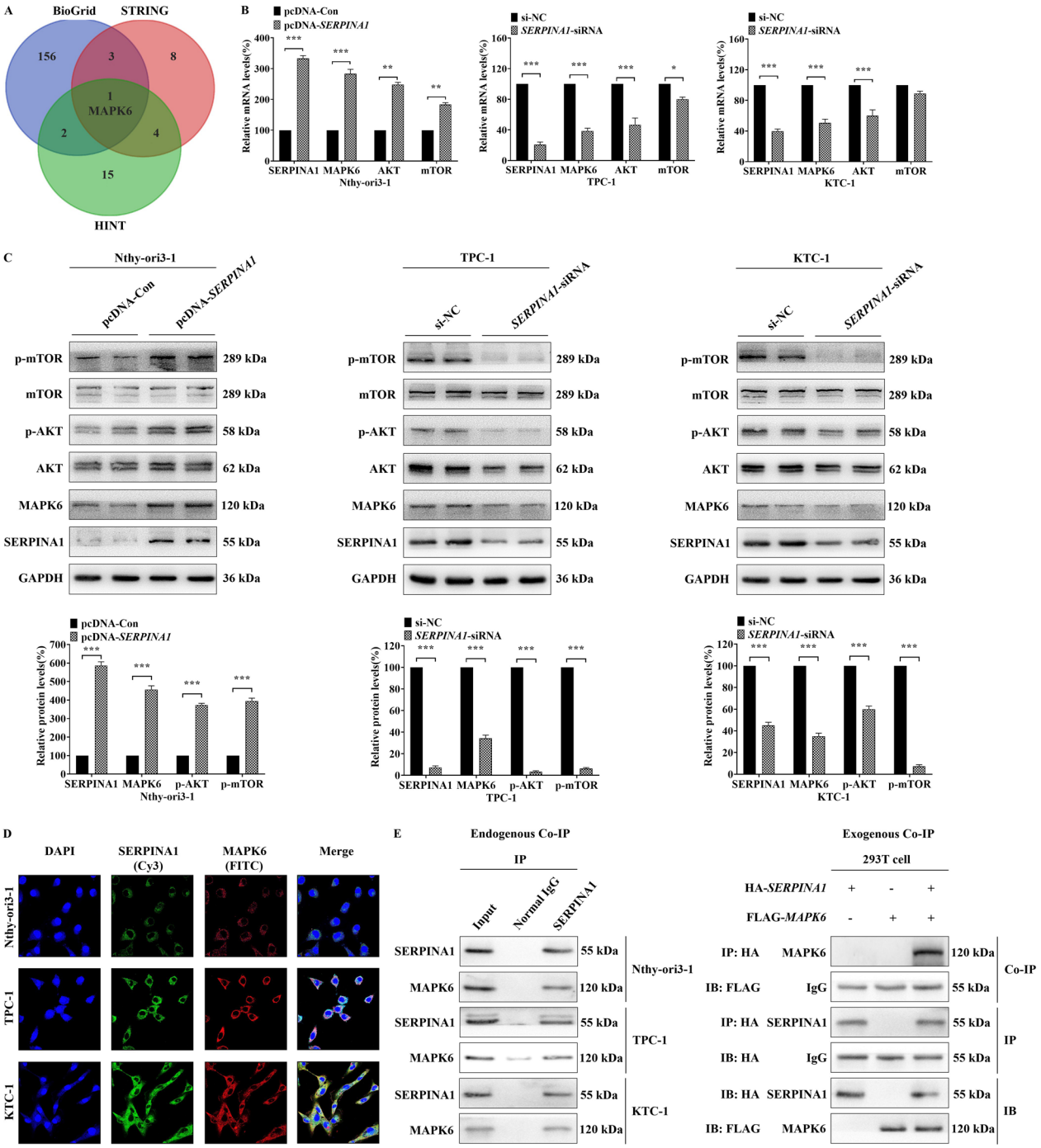

Fig. 6 SERPINA1 significantly activates the AKT/mTOR signaling pathway by directly binding to MAPK6. **A** Three protein-interacting biological information prediction websites (BioGrid, STRING and HINT) were searched for proteins that had targeted binding sites to SERPINA1 in humans. The Venn diagram showed MAPK6 as a binding partner for SERPINA1. **B**, **C** Nthy-ori3-1 (normal thyroid epithelial cell line) cells were transfected with pcDNA-Con (negative control) or pcDNA-*SERPINA1*, while TPC-1 and KTC-1 (papillary thyroid carcinoma cell lines) cells were transfected with si-NC (negative control) or *SERPINA1*-siRNA. The mRNA levels of *SERPINA1*, *MAPK6*, *AKT* and *mTOR* gene in Nthy-ori3-1, TPC-1 and KTC-1 cells were determined by qRT-PCR (B). The protein levels of SERPINA1, MAPK6, p-AKT and p-mTOR in Nthy-ori3-1, TPC-1 and KTC-1 cells were examined by Western Blot, and the relative protein expression were determined (C). Densities of bands were quantified by Image J software. GAPDH served as control. **D** SERPINA1 (Cy3: green) and MAPK6 (FITC: red) were well colocalized in Nthy-ori3-1, TPC-1 and KTC-1 cells, and the representative confocal images of immunofluorescence were shown. Blue fluorescence indicated DAPI staining for nuclear DNA. **E** The interaction between SERPINA1 and MAPK6 was determined by co-IP experiments. The endogenous co-IP and exogenous co-IP were followed by immunoblotting (IB) with the specific antibodies as indicated. For exogenous co-IP, HEK293T cells were transiently transfected with HA-tagged SERPINA1 and Flag-tagged MAPK6. All data are presented as means ± SEM for experiments conducted in triplicate. **P* < 0.05, ***P* < 0.01, ****P* < 0.001

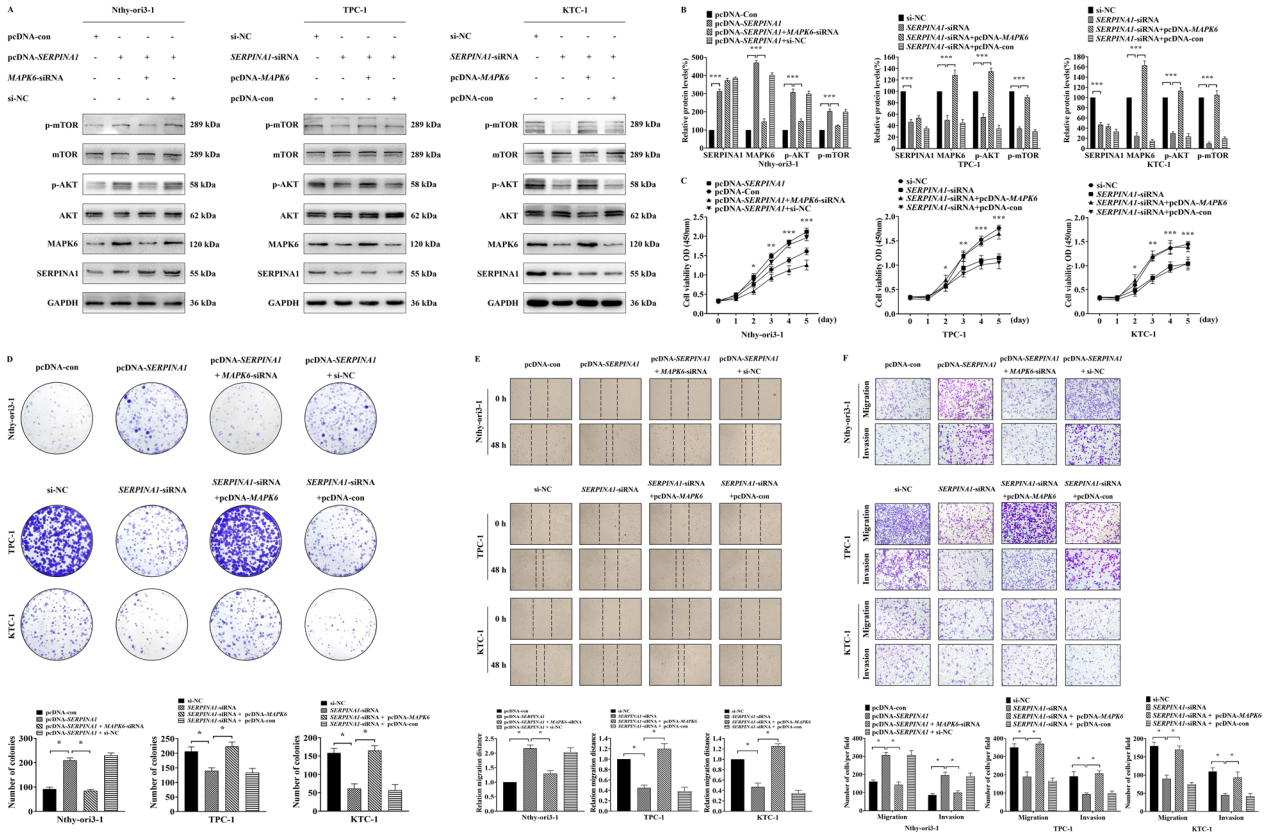

Fig. 7 SERPINA1/MAPK6/AKT/mTOR signaling pathway promotes the malignant progression of thyroid tumor cells. Nthy-ori3-1 cells were transfected with pcDNA-Con (negative control) or pcDNA-*SERPINA1* alone, or co-transfected with pcDNA-*SERPINA1* and *MAPK6*-siRNA or pcDNA-*SERPINA1* and si-NC. TPC-1 and KTC-1 cells were transfected with si-NC (negative control) or *SERPINA1*-siRNA alone, or co-transfected with *SERPINA1*-siRNA and pcDNA-*MAPK6* or *SERPINA1*-siRNA and pcDNA-Con. **A** The protein levels of SERPINA1, MAPK6, p-AKT and p-mTOR in Nthy-ori3-1, TPC-1 and KTC-1 cells were detected by Western Blot, and **B** the relative protein expression were determined. Densities of bands were quantified by Image J software. GAPDH served as control. **C** The proliferation efficiency of Nthy-ori3-1, TPC-1 and KTC-1 cells was measured by the Cell Counting Kit-8 assays. **D** The colony formation ability of cells was evaluated by a 14-day plate cloning experiment and representative pictures of colonies were displayed. Colonies between 0.3 and 1.0 mm in diameter were counted. **E** The wound healing and the relative migration distance of cells were determined. **F** The migration and invasion ability of Nthy-ori3-1, TPC-1 and KTC-1 cells were measured by Transwell assays. All data were presented as means ± SEM for experiments conducted in triplicate. *$P < 0.05$, **$P < 0.01$, ***$P < 0.001$

in PTC were significantly increased. Further AUC analysis revealed *SERPINA1* methylation had good clinical application value, which could sufficiently differentiate PTC from BTN (all above 90%), especially in combination with *BRAF* V600E (reaching 95%). These data suggest that *SERPINA1* may be a novel biomarker for early diagnosis of PTC.

Age and gender are high risk factors for thyroid disease. Among them, TC is the only malignant tumor with age as the clinical stage indicator, which is more common in young adults [43]. Moreover, TC is the only non-reproductive cancer that has a much higher incidence in women than in men. In China, the incidence of TC is three to four times higher in women than in men, and peaks at the age of 55 years [44]. Estrogen can obviously enhance the proliferative activity of thyroid cells and promote the secretion of vascular endothelial growth factor (VEGF), thus facilitating the rapid growth and malignant progression of TC [45, 46]. In this study, we found a significant association between reduced *SERPINA1* methylation and increased PTC risk, which was enhanced by female gender and younger age (age < 55 years). Furthermore, the length, size, stage and lymph node involvement of tumor are closely related to poor prognosis, recurrence and metastasis of cancer patients [47, 48]. We revealed that *SERPINA1* methylation level was lower in patients with larger tumors, advanced stages, and more lymph node involvement, suggesting that *SERPINA1* hypomethylation was closely related to malignant progression of PTC.

Although both benign and malignant thyroid tumors exhibit significant abnormalities in cell proliferation, DNA mutation and epigenetic changes, it is noteworthy that malignant tumors have a higher tendency for

recurrence and metastasis following resection [49, 50]. SERPINA1 is synthesized primarily in liver cells and released into the blood, ultimately protecting the lung from attack by elastase [51]. In addition, SERPINA1 has an immunosuppressive effect that enables the body to lose the immune surveillance of mutant cells and subsequently promotes tumorigenesis upon its elevation [52]. For example, overexpression of SERPINA1 can promote malignant progression of gastric cancer and is closely associated with poor prognosis [53]. Pancreatic cancer patients with elevated expression of SERPINA1 have a higher mortality rate [54]. Despite the strong correlation between high expression of SERPINA1 and a variety of cancers, the role of SERPINA1 in tumor cells remains poorly understood. In this study, the function of SERPINA1 was investigated in human normal thyroid epithelial cells and human PTC cells. Consistent with our findings with tissue samples from early-stage PTC cases and BTN subjects, the *SERPINA1* gene was significantly hypomethylated and overexpressed in PTC cells. Further in vitro experiments showed that overexpression of SERPINA1 could enhance the proliferation, migration and invasion of PTC cells, while knockdown of SERPINA1 decreased these capacities. Our data demonstrated that *SERPINA1* plays a tumor-driving role in the formation and development of PTC, suggesting *SERPINA1* might be a potential clinical therapeutic target for a variety of cancers, including PTC.

Although limited, potential molecular mechanisms underlying the role of *SERPINA1* in various cancers have been reported. For example, overexpression of *SERPINA1* continuously activated SMAD4/TGF-β signaling pathway, which significantly promoted the migration and invasion of gastric cancer cells [53]. Elevated plasma level of SERPINA1 activates the AKT/MAPK pathway in lung cancer cells, thereby protecting them from staurosporine-induced (bacterial lipopolysaccharide) apoptosis [55]. In addition, *SERPINA1* enhances the anti-apoptotic properties of colon cancer cells by antagonizing MEK1/2 and PI3K/AKT pathway blockers [56]. The present study is the first to investigate the specific mechanism by which SERPINA1 regulated the progression of PTC. We identified that SERPINA1 could directly bind to MAPK6. The MAPK protein family transmit signals from the cell surface to the nucleus [57]. As an atypical MAPK protein, MAPK6 phosphorylates AKT to promote tumor growth [58]. Clinically, the ineffective response to mTOR kinase inhibitors may be attributed to the MAPK6-AKT axis [24]. The MAPK/ERK pathway plays an important role in the initiation of PTC, whereas the over-activation of the PI3K/AKT carcinogenic pathway is responsible for the malignant progression of PTC [59, 60]. Notably, inhibition of MAPK6 can suppress the invasion and metastasis of breast and cervical cancers [61, 62]. Moreover, blocking the PI3K/AKT/mTOR pathway presents a potential targeted therapy for cancer [63]. Our results from normal human thyroid epithelial cells and PTC cells showed that SERPINA1 significantly activated the AKT/mTOR pathway by binding to MAPK6, thereby promoting PTC invasion and metastasis. Therefore, our studies suggest that SERPINA1/ MAPK6/ AKT/mTOR pathway contributes to the etiology of PTC.

The present study systematically investigated the clinical application value of tissue DNA methylation in the differential diagnosis of thyroid nodules in Chinese population, and it has reliable methods, rigorous design and sufficient sample size. Moreover, in vitro functional experiments demonstrated a novel tumor-driving indicator *SERPINA1* and MAPK6/AKT/mTOR signaling pathway, which enriched the understanding of PTC occurrence and development. Nevertheless, our study has limitations associated with retrospective studies. Future multicenter prospective cohort studies with larger sample size and fresh thyroid tissues are warranted to further determine the causal relationship between *SERPINA1* and PTC and to evaluate the feasibility of applying *SERPINA1* methylation in differential diagnosis of thyroid nodule in clinical practice. In addition, in vivo studies are needed to investigate the therapeutic value of targeting *SERPINA1* in PTC.

Conclusions

We revealed significant hypomethylation and overexpression of *SERPINA1* in early-stage PTC cases compared to BTN subjects by integrating the methylome and transcriptome data. Further validation with two independent case–control studies suggested that *SERPINA1* methylation might serve as a novel biomarker to distinguish PTC from BTN. Mechanistically, upregulated SERPINA1 activated AKT/mTOR pathways by binding to MAPK6 in PTC cells. Intervention of SERPINA1 or MAPK6 could significantly affect the malignancy of PTC cells. Taken together, our study suggested SERPINA1 as a diagnostic biomarker and promoted tumor progression in PTC.

Abbreviations

PTC	Papillary thyroid carcinoma
BTN	Benign thyroid nodule
5′–UTR	5′ untranslated region
MALDI-TOF	Matrix-assisted laser desorption ionization time-of-flight
ROC	Receiver operating characteristic
AUC	The area under the ROC curve
FFPE	Formalin fixed paraffin-embedded
TSH	Thyroid stimulating hormone
FT3	Free triiodothyronine
FT4	Free tetraiodothyronine
IQR	Interquartile range
OR	Odds ratio
qRT-PCR	Quantitative real-time PCR
Co-IP	Co-immunoprecipitation

CCK-8	Cell counting kit-8
SERPINA1	Serpin peptidase inhibitor, clade a (alpha-1 antiproteinase, antitrypsin), member 1
MAPK6	Mitogen-activated protein kinase 6
AKT	Protein kinase B, PKB
p-AKT	Phosphorylated protein kinase B
mTOR	Mammalian target of rapamycin
p-mTOR	Phosphorylated mammalian target of rapamycin
GAPDH	Glyceraldehyde-3-phosphate dehydrogenase
DAPI	4′,6-Diamidino-2-phenylindole
TCGA	The Cancer Genome Atlas
SEM	Standard error of mean

Supplementary Information

The online version contains supplementary material available at https://doi.org/10.1186/s13148-025-01891-3.

Supplementary material 1

Supplementary material 2

Author contributions

Author Contributions Junjie Li and Rongxi Yang designed this study; Junjie Li and Rongxi Yang wrote the main manuscript and prepared figures and tables; Junjie Li, Haixia Huang and Mengxia Li conducted experiments; Hong Li, Chenxia Jiang, Yifei Yin and Minmin Zhang were responsible for collection of samples and clinical information, data interpretation and analysis; Yizhu Mao was mainly responsible for manuscript revision. Rongxi Yang supervised and financed this study. All authors reviewed the manuscript.

Funding

This study was supported by the research funding of Nanjing Medical University, the research funding of the Jiangsu Province [Grant No. 20182020], and the 2024 Science and Technology Talent Incubation project of Zhejiang Center for Disease Control and Prevention [Grant No. 2024-A-03].

Declarations

Competing interests

The authors declare no competing interests.

Informed consent

Informed consent was obtained from all subjects involved in the study.

Author details

[1]Department of Epidemiology, School of Public Health, Nanjing Medical University, Nanjing 210000, China. [2]Zhejiang Province Center for Disease Control and Prevention, Hangzhou 310051, Zhejiang Province, China. [3]Huzhou Center for Disease Control and Prevention, 999 Changxing Road, Huzhou 313000, Zhejiang Province, China. [4]Department of Thyroid and Breast Surgery, The Affiliated Huai'an Hospital of Xuzhou Medical University and The Second People's Hospital of Huai'an, Huai'an 223000, China. [5]Department of Pathology, The Affiliated Huai'an Hospital of Xuzhou Medical University and The Second People's Hospital of Huai'an, Huai'an 223000, China. [6]Department of Pathology, The Affiliated Hospital of Nantong University, Nantong 226000, China.

Received: 26 October 2023 Accepted: 2 May 2025
Published online: 29 May 2025

References

1. Cabanillas ME, McFadden DG, Durante C. Thyroid cancer. Lancet. 2016;388(10061):2783–95.
2. Roman BR, Morris LG, Davies L. The thyroid cancer epidemic, 2017 perspective. Curr Opin Endocrinol Diabetes Obes. 2017;24(5):332–6.
3. Saravana-Bawan B, et al. Active surveillance of low-risk papillary thyroid cancer: a meta-analysis. Surgery. 2020;167(1):46–55.
4. Todsen T, et al. Ultrasound-guided fine-needle aspiration biopsy of thyroid nodules. Head Neck. 2021;43(3):1009–13.
5. Cibas ES, Ali SZ. The 2017 Bethesda system for reporting thyroid cytopathology. Thyroid. 2017;27(11):1341–6.
6. Wong LQ, Baloch ZW. Analysis of the bethesda system for reporting thyroid cytopathology and similar precursor thyroid cytopathology reporting schemes. Adv Anat Pathol. 2012;19(5):313–9.
7. Provenzano E, et al. The important role of the histopathologist in clinical trials: challenges and approaches to tackle them. Histopathology. 2020;76(7):942–9.
8. Livhits MJ, et al. Effectiveness of molecular testing techniques for diagnosis of indeterminate thyroid nodules: a randomized clinical trial. JAMA Oncol. 2021;7(1):70–7.
9. Hu MI, et al. Afirma genomic sequencing classifier and xpression atlas molecular findings in consecutive Bethesda III-VI thyroid nodules. J Clin Endocrinol Metab. 2021;106(8):2198–207.
10. Zafon C, et al. DNA methylation in thyroid cancer. Endocr Relat Cancer. 2019;26(7):R415–39.
11. Kulis M, Esteller M. DNA methylation and cancer. Adv Genet. 2010;70:27–56.
12. Constâncio V, et al. DNA methylation-based testing in liquid biopsies as detection and prognostic biomarkers for the four major cancer types. Cells. 2020;9(3):624. https://doi.org/10.3390/cells9030624.
13. Chang H, et al. DNA methylation analysis for the diagnosis of thyroid nodules - a pilot study with reference to BRAF(V) (600E) mutation and cytopathology results. Cytopathology. 2016;27(2):122–30.
14. Zhang P, et al. Targeting myeloid derived suppressor cells reverts immune suppression and sensitizes BRAF-mutant papillary thyroid cancer to MAPK inhibitors. Nat Commun. 2022;13(1):1588.
15. Su X, et al. Vitamin C kills thyroid cancer cells through ROS-dependent inhibition of MAPK/ERK and PI3K/AKT pathways via distinct mechanisms. Theranostics. 2019;9(15):4461–73.
16. Greene CM, et al. alpha1-Antitrypsin deficiency. Nat Rev Dis Primers. 2016;2:16051.
17. Yang J, et al. Identification of peptide regions of SERPINA1 and ENOSF1 and their protein expression as potential serum biomarkers for gastric cancer. Tumour Biol. 2015;36(7):5109–18.
18. Rabekova Z, et al. Alpha-1 antitrypsin and hepatocellular carcinoma in liver cirrhosis: SERPINA1 MZ or MS genotype carriage decreases the risk. Int J Mol Sci. 2021;22(19):10560. https://doi.org/10.3390/ijms221910560.
19. Zhang LY, et al. SERPINA1 methylation levels are associated with lung cancer development in male patients with chronic obstructive pulmonary disease. Int J Chron Obstruct Pulmon Dis. 2022;17:2117–25.
20. Lamartina L, et al. 8th edition of the AJCC/TNM staging system of thyroid cancer: what to expect (ITCO#2). Endocr Relat Cancer. 2018;25(3):L7–11.
21. Yang R, et al. The association between breast cancer and S100P methylation in peripheral blood by multicenter case-control studies. Carcinogenesis. 2017;38(3):312–20.
22. Lin JS, Lai EM. Protein-protein interactions: co-immunoprecipitation. Methods Mol Biol. 2017;1615:211–9.
23. Livak KJ, Schmittgen TD. Analysis of relative gene expression data using real-time quantitative PCR and the 2(-Delta Delta C(T)) Method. Methods. 2001;25(4):402–8.
24. Cai Q, et al. MAPK6-AKT signaling promotes tumor growth and resistance to mTOR kinase blockade. Sci Adv. 2021. https://doi.org/10.1126/sciadv.abi6439.
25. Coulombe P, Meloche S. Atypical mitogen-activated protein kinases: structure, regulation and functions. Biochim Biophys Acta. 2007;1773(8):1376–87.
26. Wang W, et al. MAPK4 overexpression promotes tumor progression via noncanonical activation of AKT/mTOR signaling. J Clin Invest. 2019;129(3):1015–29.
27. Grani G, et al. Contemporary thyroid nodule evaluation and management. J Clin Endocrinol Metab. 2020;105(9):2869–83.
28. Mileva M, et al. Thyroid cancer detection rate and associated risk factors in patients with thyroid nodules classified as Bethesda category III. Radiol Oncol. 2018;52(4):370–6.

29. Lai X, et al. Detection rate of thyroid nodules in routine health check-up and its influencing factors: a 10-year survey of 309 576 cases. Nan Fang Yi Ke Da Xue Xue Bao. 2020;40(2):268–73.
30. Lei Y, et al. Conventional papillary thyroid carcinoma with intraglandular lymphatic dissemination shows more aggressive features. Jpn J Clin Oncol. 2022;52(11):1311–20.
31. Wu Z, et al. Which is preferred for initial treatment of papillary thyroid cancer, total thyroidectomy or lobotomy? Cancer Med. 2021;10(5):1614–22.
32. Rodrigues MG, et al. Incidental thyroid carcinoma: Correlation between FNAB cytology and pathological examination in 1093 cases. Clinics. 2022;77:100022. https://doi.org/10.1016/j.clinsp.2022.100022.
33. Mosca L, et al. Malignancy rates for Bethesda III subcategories in thyroid fine needle aspiration biopsy (FNAB). Clinics. 2018;73:e370. https://doi.org/10.6061/clinics/2018/e370.
34. Hacim NA, et al. Impact of ultrasonographic features for thyroid malignancy in patients with Bethesda categories III, IV, and V: a retrospective observational study in a tertiary center. Cureus. 2021;13(7):e16708.
35. Zou M, et al. Concomitant RAS, RET/PTC, or BRAF mutations in advanced stage of papillary thyroid carcinoma. Thyroid. 2014;24(8):1256–66.
36. Rashid FA, et al. Prevalence of BRAF(V600E) mutation in Asian series of papillary thyroid carcinoma-a contemporary systematic review. Gland Surg. 2020;9(5):1878–900.
37. Hoeflich KP, et al. Regulation of ERK3/MAPK6 expression by BRAF. Int J Oncol. 2006;29(4):839–49.
38. Zhu G, et al. Clinical significance of the BRAFV600E mutation in PTC and its effect on radioiodine therapy. Endocr Connect. 2019;8(6):754–63.
39. Li XJ, et al. High BRAFV600E mutation frequency in Chinese patients with papillary thyroid carcinoma increases diagnostic efficacy in cytologically indeterminate thyroid nodules. Medicine (Baltimore). 2019;98(28):e16343.
40. Papanicolau-Sengos A, Aldape K. DNA methylation profiling: an emerging paradigm for cancer diagnosis. Annu Rev Pathol. 2022;17:295–321.
41. Zhang K, et al. DNA methylation alterations as therapeutic prospects in thyroid cancer. J Endocrinol Invest. 2019;42(4):363–70.
42. Brait M, et al. Correlation between BRAF mutation and promoter methylation of TIMP3, RARbeta2 and RASSF1A in thyroid cancer. Epigenetics. 2012;7(7):710–9.
43. Kazaure HS, Roman SA, Sosa JA. The impact of age on thyroid cancer staging. Curr Opin Endocrinol Diabetes Obes. 2018;25(5):330–4.
44. Wang J, et al. Thyroid cancer: incidence and mortality trends in China, 2005–2015. Endocrine. 2020;68(1):163–73.
45. Rajoria S, et al. Estrogen activity as a preventive and therapeutic target in thyroid cancer. Biomed Pharmacother. 2012;66(2):151–8.
46. Kamat A, et al. Estrogen-mediated angiogenesis in thyroid tumor microenvironment is mediated through VEGF signaling pathways. Arch Otolaryngol Head Neck Surg. 2011;137(11):1146–53.
47. Ludwig JA, Weinstein JN. Biomarkers in cancer staging, prognosis and treatment selection. Nat Rev Cancer. 2005;5(11):845–56.
48. Cserni G, et al. The new TNM-based staging of breast cancer. Virchows Arch. 2018;472(5):697–703.
49. Kim HY, et al. Clinical difference between benign and malignant tumors of the hard palate. Eur Arch Otorhinolaryngol. 2020;277(3):903–7.
50. Patel A. Benign vs malignant tumors. JAMA Oncol. 2020;6(9):1488.
51. Kohnlein T, Welte T. Alpha-1 antitrypsin deficiency: pathogenesis, clinical presentation, diagnosis, and treatment. Am J Med. 2008;121(1):3–9.
52. Schuster R, et al. Distinct anti-inflammatory properties of alpha1-antitrypsin and corticosteroids reveal unique underlying mechanisms of action. Cell Immunol. 2020;356:104177.
53. Jiang L, Hu LG. Serpin peptidase inhibitor clade A member 1-overexpression in gastric cancer promotes tumor progression in vitro and is associated with poor prognosis. Oncol Lett. 2020;20(6):278.
54. Chia-Chun W, et al. Identification of fucosylated SERPINA1 as a novel plasma marker for pancreatic cancer using lectin affinity capture coupled with iTRAQ-based quantitative glycoproteomics. Int J Mol Sci. 2021;22(11):6079. https://doi.org/10.3390/ijms22116079.
55. Schwarz N, et al. Alpha1-antitrypsin protects lung cancer cells from staurosporine-induced apoptosis: the role of bacterial lipopolysaccharide. Sci Rep. 2020;10(1):9563.
56. Ljujic M, et al. Alpha-1 antitrypsin affects U0126-induced cytotoxicity in colon cancer cell line (HCT116). Mol Biol (Mosk). 2016;50(1):174–8.
57. Burotto M, et al. The MAPK pathway across different malignancies: a new perspective. Cancer. 2014;120(22):3446–56.
58. Liang J, et al. HNF4G increases cisplatin resistance in lung adenocarcinoma via the MAPK6/Akt pathway. PeerJ. 2023;11:e14996.
59. Chen L, Zhuo D, Yuan H. Circ_100395 impedes malignancy and glycolysis in papillary thyroid cancer: Involvement of PI3K/AKT/mTOR signaling pathway. Immunol Lett. 2022;246:10–7.
60. Zheng T, et al. MiR-30c-5p loss-induced PELI1 accumulation regulates cell proliferation and migration via activating PI3K/AKT pathway in papillary thyroid carcinoma. J Transl Med. 2022;20(1):20.
61. Zhang M, et al. miR-653-5p suppresses the growth and migration of breast cancer cells by targeting MAPK6. Mol Med Rep. 2021. https://doi.org/10.3892/mmr.2021.11839.
62. Huang Y, et al. Rab31 promotes the invasion and metastasis of cervical cancer cells by inhibiting MAPK6 degradation. Int J Biol Sci. 2022;18(1):112–23.
63. Yu L, Wei J, Liu PD. Attacking the PI3K/Akt/mTOR signaling pathway for targeted therapeutic treatment in human cancer. Semin Cancer Biol. 2022;85:69–94.

Publisher's Note